Journal of Applied Electrochemistry **31**: 1071–1077, 2001.

Electrodeionization 2: The migration of nickel ions absorbed in a flexible ion-exchange resin

P.B. SPOOR[1], W.R. TER VEEN[2], L.J.J. JANSSEN[1]
[1]*Eindhoven University of Technology, Department of Chemical Engineering, Laboratory of Process Development, PO Box 513, 5600 MB Eindhoven, The Netherlands*
[2]*TNO Institute of Environmental Sciences, Energy Research and Process Innovation, Laan van Westenenk 501, PO Box 342, 7300 AH Apeldoorn, The Netherlands*

Received 19 February 2001; accepted in revised form 12 June 2001

Key words: deionization, electrodialysis, ion exchange, nickel

Abstract

The removal of nickel ions from a low cross-linked ion-exchange resin using an applied electrical potential gradient was studied. The potential gradient across a bed of ion-exchange particles, in which nickel ions were absorbed, was varied by two methods. One involved a change of cell voltage across beds of constant width, the other a change of bed width at constant cell voltage. In this way, various characteristics concerning the electrodialytic regeneration of a bed of ion-exchange particles in the nickel form were ascertained. The diffusion coefficient, current efficiency and migration rate of nickel in the bed are discussed. It is shown that the current efficiency for the removal of nickel is nearly one hundred percent when the bed is in the nickel form, and that the rate of regeneration is proportional to the cell voltage.

List of symbols

A_{bed}	area of the ion exchange bed perpendicular to the potential gradient (m^2)
$\overline{c}_i$	concentration of species i (mol m^{-3})
$\overline{c}_i^0$	initial concentration of species i (mol m^{-3})
$\overline{D}_{i,\text{eff}}$	apparent diffusion coefficient of species i in ion-exchange bed (m^2 s^{-1})
$D^0_{i,\text{eff}}$	apparent initial diffusion coefficient of species i in ion-exchange bed (m^2 s^{-1})
d_{bed}	width of ion-exchange bed (m)
ΔE	potential difference (V)
F	faradaic constant (C mol^{-1})
I	current (A)
k_{m}	mass-transfer rate coefficient (s^{-1})
N_i	flux of species i (mol m^{-2} s^{-1})
N_i^0	initial flux of species i (mol m^{-2} s^{-1})
n_i	quantity of species i (mol)
Q_{e}	charge passed through cell (C)
R	gas constant (J mol^{-1} K^{-1})
T	temperature (K)
t	time (s)
V	volume (m^3)
X_i	fraction of species i in ion-exchange bed (dimensionless)
z	valence (dimensionless)
η	current efficiency (%)
grad φ	electrical potential gradient

Subscripts

a	anode compartment
bed	bed of ion-exchange resin occupying centre compartment
cell	entire cell including anode, cathode and centre compartments
i	ionic species
k	cathode compartment
m	membrane
8h	quantity obtained after 8 h electrodialysis time

1. Introduction

This work deals with the electrodialytic regeneration of a low cross-linked, flexible ion-exchange material in which nickel ions are absorbed. This complements previous work; a macroporous resin with a high degree of cross-linking (Amberlyst 15) was investigated in [1]. The present considers the influence of the voltage gradient over the ion-exchange bed on the migration of nickel through the system.

The migration of ions through the ion-exchange resin is governed by various parameters. One such parameter is the apparent (or effective) diffusion coefficient of absorbed ions in the ion-exchange particles. The apparent diffusion coefficient of nickel ions inside an ion-exchange particle, $\overline{D}_{\text{Ni,eff}}$, is affected by the state of the

ion-exchange resin. $\bar{D}_{Ni,eff}$ increases if the competing absorbed ions have higher diffusion coefficients, and decreases if they are lower. This occurs because the type of ions absorbed by the resin affect its water content; that is, the resin will contain a lower fraction of water in the Ni^{2+} form compared to that of the H^+ form. If the water content of the resin is low, the mobility of absorbed ions will be small [2].

This work studies a resin of low cross-linking, namely the Dowex brand 50WX-2 ion-exchange resin. Its low degree of cross-linking allows it to take up a higher fraction of water and the absorbed ions therefore display higher conductivities when compared to resins of higher cross-linking. The ion exchange bed can therefore be regenerated in a time shorter than that of more highly cross-linked resins. The use of a low cross-linked resin, however, produced problems resulting from a strong degree of swelling that occurred as Ni^{2+} was replaced by H^+ upon regeneration. Consequently, the concentration of fixed sites, $\bar{D}_{Ni,eff}$, and the pressure drop over the cell in the solution flow direction were no longer constant.

2. Experimental details

2.1. *Conversion of the Dowex 50X-2 ion-exchange resin to the Ni^{2+} form*

Preparation of the nickel-loaded resin involved the following steps:

(i) Initial regeneration of the ion-exchanger (1.50×10^{-4} m^3 as received) with two bed volumes of 2 M H_2SO_4. This procedure was repeated twice.
(ii) Rinsing of the exchanger with deionized water until the effluent was pH neutral.
(iii) Equilibration and storage of the exchanger in 3.00×10^{-4} m^3 deionized water.
(iv) The water was filtered off and the resin equilibrated in 1.50×10^{-4} cm^3 1.3 M $NiSO_4$ for 1 day.
(v) The resulting nickel loaded resin (1.08×10^{-4} m^3) was washed and stored in 4.00×10^{-4} m^3 deionized water to remove any sorbed electrolyte. The retenate was then analysed by AAS for Ni^{2+} content.

This procedure produced an essentially fully loaded resin with a nickel concentration of 602 mol m^{-3} wet settled bed.

2.2. *Experimental set-up*

The experimental set-up described in [1] was used. The vertical electrolysis cell had three compartments: a central compartment that contained the bed of ion-exchange particles as well as the anode and cathode compartments that contained the electrolyte solutions (Figure 1). The three compartments were separated using an anion selective membrane on the anode side and a cation selective membrane on the cathode side. It is possible to use an anion selective membrane in this cell as long as the concentration of acid in the anolyte is high (i.e., >1 M) [1]; the choice to use such a membrane is based on the fact that future cell designs may be

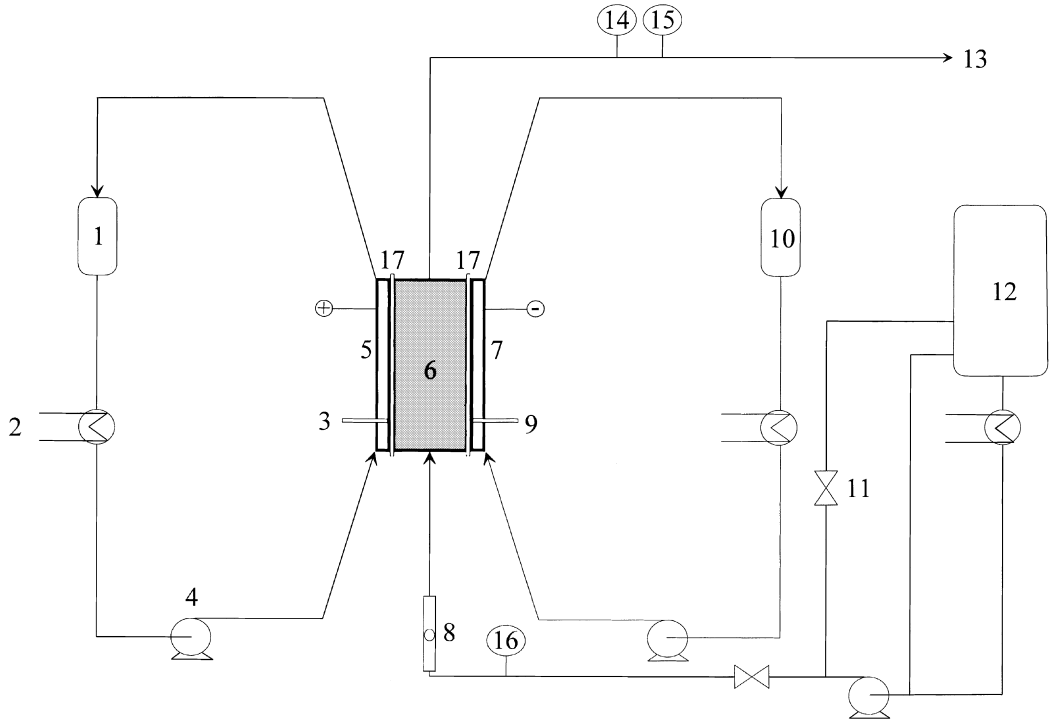

Fig. 1. Experimental set-up (cell enlarged for clarity): (1) anode reservoir; (2) heat exchanger; (3) reference [1]; (4) pump; (5) anode compartment; (6) centre compartment; (7) cathode compartment; (8) flow meter; (9) reference [2]; (10) cathode reservoir; (11) valve; (12) feed reservoir; (13) to waste container; (14) pH cell; (15) conductivity cell; (16) conductivity cell; (17) ion-selective membrane.

required to remove anions and/or to allow for a stack of columns similar to that found in conventional electrodialysis.

An aliquot of the nickel-loaded resin prepared in Section 2.1 was placed in the centre compartment of the cell for each run. Deionized water from a 0.03 m^3 reservoir was passed once through the ion-exchange compartment bottom up at a flow rate of 4.2×10^{-7} m^3 s^{-1} while 0.1 M H_2SO_4 solutions were circulated through the outer compartments with a flow rate of approximately 1.1×10^{-5} m^3 s^{-1}. The deionized water supplied to the ion-exchange compartment as well as the solutions in the outer compartments were kept at a constant temperature of 298 K. A constant cell voltage was applied using a Delta Elektronika Power Supply D 050-10. During the course of the experiments the following characteristics were monitored: current (Keithley 177 Microvolt DMM); cell voltage (Multilab computer interface); charge passed through the cell (Wenking E VI80 voltage integrator); inlet and outlet feed solution conductivity, (Radiometer Type CDM 2d) and pH of solution (Philips PW 9414) at the outlet of the centre compartment; and temperature of all three solutions at the outlet of each compartment (Hg thermometer).

Samples of the cathode compartment solution (1 cm^3) were taken on an hourly basis and analysed for nickel content using flame atomic adsorption (Perkin Elmer 3030). The initial ohmic drop across the cell was measured using an Eco-Chemie system with PGSTAT 20.

Transport experiments were carried out at constant bed width (15 mm) and various cell voltages; that is, 0, 5, 10, 20, 30 and 40 V. Another series of experiments was carried out at constant cell voltage (30 V) and various bed widths; that is, 5, 10, 15 and 20 mm. In addition to these, an experiment was carried out during which the cell voltage was increased periodically. A 15 mm wide centre compartment was used and the entire experiment lasted a total of 12 h. The cell voltage was constant at 5 V for the first 4 h, 20 V for the next 4 and 40 V for the remaining 4 h.

3. Results

3.1. *Effect of cell voltage*

Experiments were completed in which different voltages were applied across a cell containing Dowex 50WX-2 initially loaded with 602 mol m^{-3} Ni^{2+}. The diffusion of nickel into the cathode compartment, excluding transport due to migration, occurred in the experiment without an applied cell voltage. This process involved the exchange of nickel from the ion-exchange particles with hydrogen from the catholyte. During the experiments with an applied cell voltage, a front of absorbed nickel ions was observed to move across the bed towards the cathode compartment. It was observed as a green–yellow boundary. At the end of the 8 h experiments with cell voltages greater than 10 V, this front had completely disappeared, returning the exchanger to its original light yellow colour indicative of its hydrogen form.

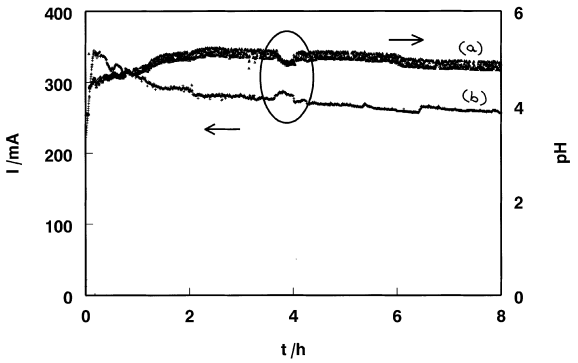

Fig. 2. Current and pH change over time for the 20 V experiment in which a bed of Dowex 50X-2 particles in the nickel form was regenerated: (a) pH; (b) current.

Characteristic results for the current and effluent pH over time are depicted in Figure 2. A sudden decrease in the flow rate from 4.2×10^{-7} to approximately 2×10^{-7} m^3 s^{-1} for a period of about 0.5 h resulted in a clear decrease in effluent pH and an increase in current (i.e., circled region of Figure 2). Thereafter, the flow rate was adjusted to the original level, i.e. 4.2×10^{-7} m^3 s^{-1}. The pH of the centre compartment solution decreased due to the diffusion of acid from the anode compartment [1, 3–5]. At lower solution flow rate, the conductivity of the centre compartment solution increased, causing a corresponding increase in current.

The quantity of Ni^{2+} transported from the centre compartment into the cathode compartment, $n_{Ni,k}$, as a function of time is shown in Figure 3. From this Figure it follows that the rate of nickel transport decreased over the course of the experiments and the rate of nickel transport increased with increasing cell voltage.

During the experiment with $\Delta E = 40$ V, $n_{Ni,k}$ decreased after $t = 3$ h. This was caused by the deposition of metallic nickel on the cathode. A negligible quantity

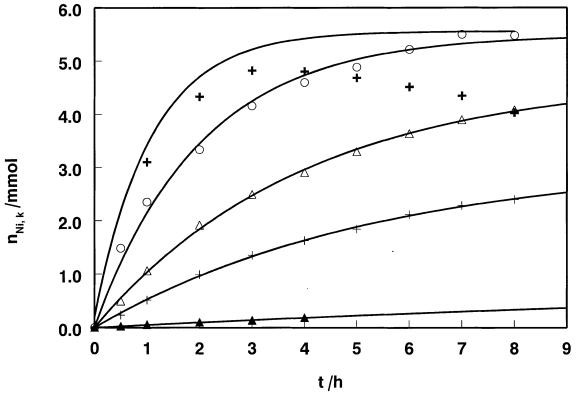

Fig. 3. Nickel content in catholyte over time for various cell voltages. A bed of Dowex 50X-2 particles initially in the nickel form was used in all cases: (▲) 0; (+) 5; (△) 10; (◯) 20; (+) 40 V.

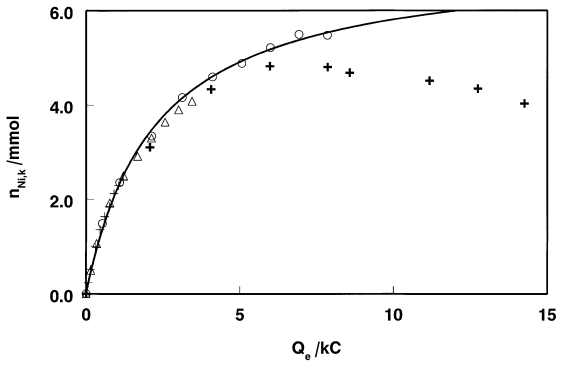

Fig. 4. Nickel quantity in catholyte with respect to the charge passed through the cell for various cell voltages and a constant bed width of 15 mm: (+) 5; (△) 10; (◯) 20; (+) 40 V.

of Ni^{2+} was deposited during the 20 V experiment while no nickel deposition was found in either the 5 or 10 V experiments; the deposition of nickel is a function of current density and catholyte concentration. The data sets were fitted using the following exponential equation:

$$n_{Ni,k} = n_{Ni,k,8h}(1 - e^{-k_m t}) \quad (1)$$

where $n_{Ni,k,8h}$ is determined experimentally and represents the quantity of nickel in the cathode compartment at the end of the experiment, and k_m is the calculated apparent mass transfer rate coefficient. Figure 3 shows that Equation 1 agrees with the experimental results and it will later be shown that the value k_m is directly proportional to the cell voltage.

The relationship between the charge passed through the cell, Q_e, and the quantity of nickel ions removed from the bed, $n_{Ni,k}$, is given in Figure 4. This demonstrates that the $n_{Ni,k}$ against Q_e relation does not depend on the cell voltage. Only under conditions where nickel metal deposition occurs does a deviation in the relationship exist.

In addition to these experiments, a single experiment was run during which the cell voltage was increased every 4 h. Figure 5 depicts the amount of nickel in the catholyte during the experiment. From this it can be seen that directly after every voltage increase an increase in $n_{Ni,k}$ occurred. The data pertaining to each E_{cell} were fitted using Equation 1.

3.2. *Effect of bed width*

The effect of bed width on the migration rate of Ni^{2+} was studied at a constant cell voltage of 30 V; the initial current densities averaged approximately 24.5 mA cm^{-2} and increased to an average of 30.4 mA cm^{-2} after the 8 h electrodialysis. The quantity of Ni^{2+} transported to the cathode compartment as a function of the electrodialysis time is shown in Figure 6. Here the slopes of the curves demonstrate that the Ni^{2+} migration rate decreased with electrodialysis time and declining bed width. These sets of data were found to follow the same exponential pattern as the data in Section 3.1 and were fitted using Equation 1. The 5 mm bed, in which $n_{Ni,k}$ = 3.0 mmol after the 8 h of electrodialysis, was almost completely regenerated while the 20 mm bed, with $n_{Ni,k}$ = 8.6 mmol after 8 h of electrodialysis, was 70% regenerated.

The quantity of nickel in the catholyte is depicted with respect to charge, Q_e, in Figure 7. This reveals that an increase in bed width caused a decrease in the charge required to remove a given amount of nickel. It follows that the fraction of hydrogen transport during the 8 h electrodialysis experiments was greater for beds of smaller width; this was due to the increased rate at which they were regenerated.

4. Discussion

The nickel flux from the bed of ion-exchange resin was calculated using the derivative of Equation 1:

$$N_{Ni} = \frac{dn_{Ni,k}}{A_{bed}dt} = \frac{k_m n_{Ni,k,8h}}{A_{bed}} e^{-k_m t} \quad (2)$$

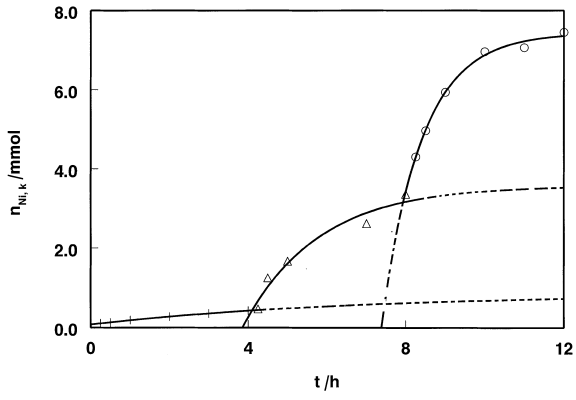

Fig. 5. Nickel quantity in catholyte as a function of time for the experiment in which ΔE_{cell} was increased every 4 h. A bed of Dowex 50X-2 particles initially in the nickel form was used. Cell voltage was varied: (+) 5; (△) 20; (◯) 40 V.

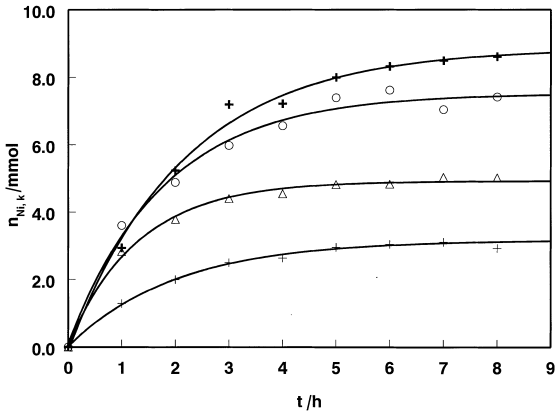

Fig. 6. Nickel quantity in catholyte over time for the series of experiments in which the bed width was varied. A constant cell voltage of 30 V was applied and a bed of Dowex 50X-2 particles initially in the nickel form was used: (+) 5; (△) 10; (◯) 15; (+) 20 mm.

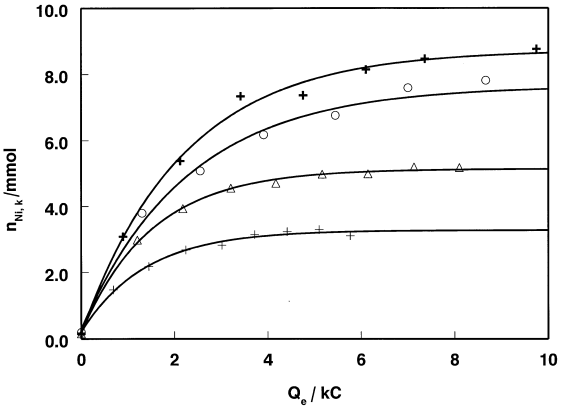

Fig. 7. Nickel quantity in the catholyte as a function of charge for the Dowex resin initially in the nickel form and at various bed widths: (+) 5; (△) 10; (◯) 15; (+) 20 mm.

It was found that N_{Ni} decreased exponentially with time; this was due to the decreasing concentration of nickel in the resin. The initial nickel flux is given by

$$N^0_{Ni} = \frac{k_m n_{Ni,k,8h}}{A_{bed}} \tag{3}$$

The initial flux, N^0_{Ni}, is of interest as it represents the flux before any concentration gradients and swelling effects were produced in the bed.

A plot of N^0_{Ni}, obtained from the results of Figure 3 and Equation 3, is depicted in Figure 8 as a function of bed voltage drop, ΔE_{bed}, at constant bed width, where

$$\Delta E_{bed} = E_{cell} - (E_{anode} + E_{cathode} + \Delta E_{m1} + \Delta E_{m2} + \Delta E_k + \Delta E_a) \tag{4}$$

The electrode potentials were determined from analyses of I/E curves and are together approximately 1.8 V. The potential drop across the membranes were calculated using resistances presented in [1] and the potential drop over the electrolytes were calculated using resistances given in literature [6]. This graph illustrates the linear relationship between the initial nickel fluxes and the bed potential difference. It is in agreement with the migration term of the Nernst–Planck equation [2].

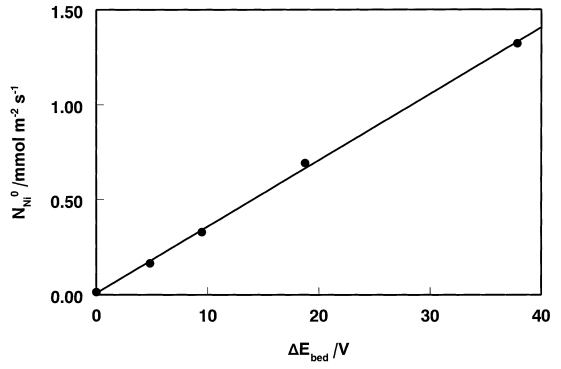

Fig. 8. Initial nickel flux into the cathode compartment with respect to cell voltage for the series of experiments with a constant bed width, (15 mm) and variable cell voltage (●).

It is possible to calculate the apparent diffusion coefficient of nickel in the bed, $\overline{D}_{Ni,eff}$, using $\overline{N}^0_{Ni}$, $\bar{c}^0_{Ni}$ and the migration term of the Nernst–Planck equation, where

$$N^0_{Ni} = z_{Ni}\bar{c}^0_{Ni}\frac{\overline{D}^0_{Ni,eff}F}{RT}\,\mathrm{grad}\,\varphi \tag{5}$$

The average $\overline{D}^0_{Ni,eff}$ was calculated for the experiments with a constant bed width. It was found to be $(1.13 \pm 0.04) \times 10^{-11}$ m^2 s^{-1} for Dowex 50X-2 loaded with nickel. This information can be used to determine the characteristics of a continuous deionization process [7], such as bed area, solution flow rate and bed potential difference, for the processing of a dilute nickel solution.

The relationship between the quantity of nickel transported to the cathode compartment and the quantity of charge used during electrodialysis is a measure of the efficiency of nickel transport under an applied potential difference. Figure 4 establishes this relationship as being independent of the potential drop over the cell at constant bed width. This means that the current efficiency for nickel transport, η_{Ni}, given by

$$\eta_{Ni} = \frac{2F(n^{t2}_{Ni,k} - n^{t1}_{Ni,k})}{Q^{t2}_e - Q^{t1}_e} \tag{6}$$

is independent of the potential drop over the bed when the bed width is kept constant. Although the current efficiency does not show a dependence on the potential drop over the bed, it is dependent on the bed width (Figure 7). The slope of a curve in Figure 7 represents the current efficiency of the system. It can be seen that the current efficiency for nickel removal increased with bed width; after the 1 h electrodialysis they were 36, 45, 53 and 63% for the 5, 10, 15 and 20 mm beds, respectively, and decreased exponentially to nearly zero. The increase in current efficiency with bed width was due to the increasing quantity of nickel in the centre compartment (along the axis of migration) available for transport. Due to the increased quantity of nickel along the axis of migration, a smaller quantity of H^+ ions originating at the anode side of the cell 'broke through' the nickel form of the bed to the catholyte in the time frame observed. The $n_{Ni,k}$ against Q_e curves presented in Figures 4 and 7 represent the transport of nickel with the effect of time removed; it can therefore be said that, at constant bed width (Figure 4), the cell voltage only affects the time required for regeneration (i.e., the rate of regeneration is proportional to the cell voltage). This is true only at early electrodialysis times in Figure 7, again because of the differing quantities of nickel in beds of varying width. To determine this effect, the initial quantity of nickel in the bed was taken into account by plotting $n_{Ni,k}/\bar{n}^0_{Ni}$ against $Q_e/2F\bar{n}^0_{Ni}$ (Figure 9). By comparing Figure 9 to Figure 7 it can be seen that once $\bar{n}^0_{Ni}$ is taken into account, the curves no longer show a dependence on bed width. The fraction of

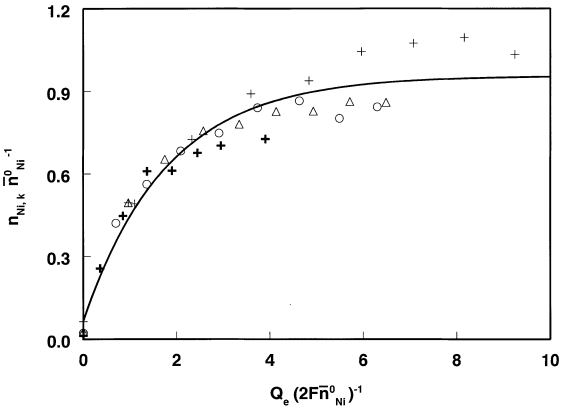

Fig. 9. Fraction of nickel removed from the bed vs. the ratio of charge passed through the bed, Q_e, and the initial charge of Ni^{2+} in the nickel loaded Dowex ion-exchange beds with widths: (+) 5; (△) 10; (◯) 15; (+) 20 mm.

nickel removed from the beds after a fixed quantity of charge is passed through the beds is therefore proportional to the potential drop over the bed and the initial quantity of nickel in the bed.

A similar experiment utilizing a bed of highly cross-linked Amberlyst 15 particles was carried out in [1]. In this case the $n_{Ni,k}/Q_e$ relation did not depend on the bed width at constant cell voltage. This was due to the small degree of bed regeneration during these experiments. At low degrees of bed regeneration the fraction of nickel in the ion-exchanger was essentially uniform throughout the bed. Under these circumstances, the bed width does not considerably affect the transport of nickel to the catholyte.

The logarithm of η_{Ni} is plotted in Figure 10 as a function of the fraction of Ni^{2+} removed from the bed ($n_{Ni,k}/\bar{n}^0_{Ni}$) for experiments at various cell voltages and constant bed width. A linear fit of this trend gives an intercept of approximately zero. This represents a current efficiency of approximately 100% for the transport of Ni^{2+} when the exchanger is at capacity.

A clear increase in the flux of nickel ions was observed with increasing cell voltage; this increase was found to be directly proportional to the cell voltage in Figures 4 and 8. The relationship between nickel flux and the cell voltage increase during the course of an experiment has not yet been shown. By analysing the slopes of the curves in Figure 5, the flux directly after the increase in cell voltage, at $t = 4$ and 8 h, is approximately 20 times that of the flux just before the increases. This large increase may be attributed to the different concentration gradients and their affect on the potential distribution in the bed.

A comparison between the two series of experiments described in Sections 3.1 and 3.2 was made using Equation 1; this equation contains two factors, k_m and $n_{Ni,k,8h}$. In Figure 11 these parameters are represented for both series of experiments as a function of the mean bed potential gradient, $\Delta E_{bed}/d_{bed}$. Since the rate of nickel removal was affected by the initial quantity of nickel in the bed, $k_m/\bar{n}^0_{Ni}$ was plotted against $\Delta E_{bed}/d_{bed}$. In this Figure $k_m/\bar{n}^0_{Ni}$ is seen to increase linearly with the mean potential difference over the bed. The apparent mass transfer rate constant, and hence the bed regeneration rate, is directly proportional to the mean potential difference over the bed and the initial quantity of nickel in the bed for both series of experiments. The value of k_m at a mean bed potential of zero represents the diffusion process only. The diffusion of nickel ions to the catholyte occurred due to the exchange of H^+ from the catholyte with Ni^{2+} from the ion-exchange bed and involves no net charge transfer.

Figure 11 also depicts $X_{Ni,8h}$, the fraction of nickel remaining in the bed at the end of the 8 h electrodialysis, where

$$X_{Ni,8h} \equiv 1 - \frac{n_{Ni,k,8h}}{\bar{n}^0_{Ni}} \tag{7}$$

$X_{Ni,8h}$ was found to decrease exponentially with the mean potential difference over the bed. From this Figure it follows that the two series of experiments produced comparable results that showed the dependence of regeneration rate on both cell voltage and bed width. No large discrepancies were observed within the range of cell voltages and bed widths studied. Smaller discrep-

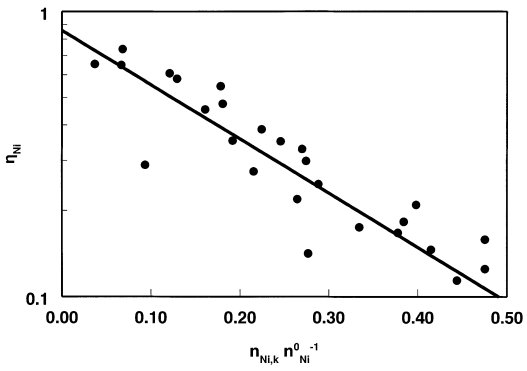

Fig. 10. Logarithm of differential current efficiency as a function of the fraction of nickel removed from the bed. Current efficiencies for transport after nickel deposition had begun were not included. Current efficiencies are shown for experiments run with a constant bed width (15 mm) and variable cell voltage (●).

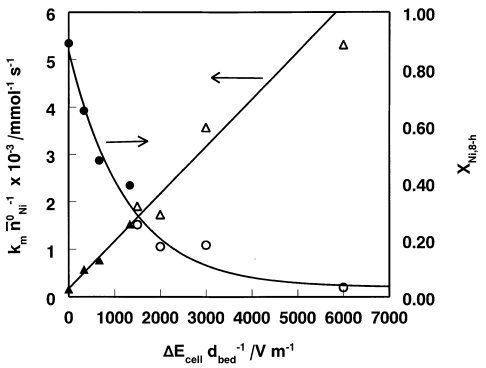

Fig. 11. $k_m\bar{n}^{0-1}_{Ni}$ and $X_{Ni,lim}$ values plotted against $\Delta E d^{-1}_{bed}$ for experimental series 3.1 at various cell voltages and series 3.2 with various bed widths. $k_m\bar{n}^{0-1}_{Ni}$: (▲) series 3.1, (△) series 3.2; $\bar{x}_{Ni,lim}$: (●) series 3.1, (◯) series 3.2.

ancies in the results pertaining to the various bed widths can be attributed to artefacts such as the solution pressure drop across the bed and membrane bulging (the bed width, d_{bed}, was assumed equal to the width of the central compartment), the effects of which would increase with decreasing bed width.

5. Conclusions

The flux of nickel through an ion-exchange resin is dependent on the potential gradient and the Ni^{2+} ionic fraction in the particle. It was found that the regeneration rate of a bed of ion-exchange particles loaded with Ni^{2+} is directly proportional to the potential difference across a bed of ion-exchange particles; this is in agreement with the migration term of the Nernst–Planck equation. To compare the entire length of the experiments, a single apparent rate constant, along with the initial quantity of nickel in the bed (unit of $mmol^{-1}\ s^{-1}$) and the fraction of nickel remaining in the bed at the end of the 8 h experiments, were plotted against the mean bed potential difference. A good agreement between all experiments was found.

An abrupt increase in the potential gradient across the bed at later electrodialysis times caused a disproportionately large increase in N_{Ni}. It is believed that this was due to concentration gradients in the bed and their effect on the distribution of potential drop over the bed.

The current efficiency for nickel transport, η_{Ni}, was found to decrease with decreasing ionic fraction of nickel in the resin. It was also found to have a value of about 1 when the bed was completely in the nickel form. The initial apparent diffusion coefficient of nickel in the bed was determined to be $1.13 \times 10^{-11}\ m^2\ s^{-1}$; this is of the same order of magnitude as the self-diffusion coefficient of other divalent metals through an ion-exchange resin of the same type [8]. The apparent diffusion coefficient is of practical importance as it can be used to determine the system requirements, such as bed area and cell voltage, needed to process a nickel solution under various conditions.

References

1. P.B. Spoor, W.R. ter Veen and L.J.J. Janssen, *J. App. Electrochem.* **31** (2001) 523–553.
2. F. Helfferich, 'Ion Exchange' (McGraw-Hill, London, 1961).
3. J. Molenat, G. Pourcelly and I. Tugas, C. Gavach, *Russian J. Electrochem.* **32** (1996) 170.
4. Y. Lorrain, G. Pourcelly and C. Gavach, *J. Membrane Sci.* **110**, (1996) 181–190.
5. Y. Lorrain, G. Pourcelly and C. Gavach, *Desalination* **109** (1997) 231–239.
6. R. Parsons, 'Handbook of Electrochemical Constants' (Butterworths Scientific, London, 1959).
7. P.B. Spoor, L. Koene, W.R. ter Veen and L.J.J. Janssen, paper to be published in the *Chem. Eng. J.*
8. G.E. Boyd and B.A. Soldano, *J. Am. Chem. Soc.* **75** (1953) 6091.